ENF SIGNAL EXTRACTION FOR ROLLING-SHUTTER VIDEOS USING PERIODIC ZERO-PADDING

Jisoo Choi and Chau-Wai Wong

North Carolina State University, Raleigh, USA

ABSTRACT

Electric Network Frequency (ENF) analysis is a promising forensic technique for authenticating digital recordings and detecting tampering within the recordings. The validity of ENF analysis heavily relies on high-quality ENF signals extracted from multimedia recordings. In this paper, we propose an ENF signal extraction method for rolling shutter acquired videos using periodic zero-padding. Our analysis shows that the extracted ENF signals using the proposed method are not distorted and the component with the highest signal-to-noise ratio is located at the intrinsic frequency. The experimental results show that our proposed method can generate more precise ENF signals than those from the state-of-the-art method.

Index Terms— Electric Network Frequency (ENF) signal, frequency estimation, multirate analysis, rolling shutter

1. INTRODUCTION

Electric Network Frequency (ENF) analysis is a promising forensic technique for authenticating digital recordings [1] and detecting tampering within the recordings [2]. The ENF is the supply frequency of an electric grid. The supply frequency is not constant, but fluctuates along the time around its nominal value of 60 Hz in North America or 50 Hz in most other regions of the world, due to the mismatch between the demand and the supply within the power network. Since different nodes within the grid are interconnected, the fluctuations in frequency at different locations of the same grid share similar patterns. The instantaneous values of ENF over time are regarded as the ENF signal, which can serve as a natural time stamp for authenticating multimedia recordings.

The ENF signal can be embedded into audio recordings via sensing acoustic vibrations or via interfering electromagnetically in sensing circuits [1]. Studies in [1,3–6] show that ENF traces extracted from audio recordings can be used to assess the authenticity of the recordings. Studies in [7,8] show that ENF extracted from the audio track of videos can be used to identify the locations that videos were recorded. The study in [9] shows that the ENF analysis can be extended beyond the realm of the forensic science to multimedia signal processing, e.g., the synchronization of videos without overlapped scenes, and the alignment of historical audio recordings.

More recent studies revolve around extracting ENF traces from the visual track of multimedia recordings [10–12]. Indoor lightings, such as fluorescent lights and incandescent bulbs, vary their light intensity at a frequency twice of that of the supply voltage, leading to near-invisible flickering in the illuminated environment. Consequently, cameras under the indoor illumination environment may capture videos that contain ENF signals. One of the major concerns encountered in extracting the embedded ENF signal from visual tracks is the aliasing effect due to limited sampling rate [10]. Specifically, when the nominal value of the ENF and the frame rate are 60 Hz and 30 frames per second (fps), respectively, it is challenging to extract the aliased ENF component because it is overlaid with the DC frequency component.

To tackle the issue of the limited sampling rate, the authors in [10, 11] demonstrated that the rolling shutter mechanism, which is traditionally considered detrimental in image and video analysis, can be exploited to increase the effective sampling rate. The rolling shutter acquires a video by sequentially reading and storing the pixel values of horizontal lines of each landscape frame. Since successive lines of a frame are acquired at different time points, the rolling shutter can foster the ENF signal extraction from the visual track by increasing the effective sampling rate by a factor of the number of lines [10]. In [11], the authors proposed an extraction method that directly concatenates the row signals of all frames by ignoring the idle periods occurred at the end of each frame. Multirate signal analysis was applied to show that the extracted signal approximates the desired ENF signal.

In this paper, we conduct a further study on exploiting the rolling shutter and propose a periodic zero-padding method for extracting the exact, undistorted ENF signals from the visual track. The proposed extraction method conducts an equivalently uniform sampling along the time by returning zeros during the idle period at the end of each frame. Our analysis will show that the spectrogram around the frequency of interest is not distorted and the component with the highest signal-to-noise ratio is located at the intrinsic frequency.

The rest of the paper is organized as follows. In Section 2, we describe and analyze the proposed method for ENF signal extraction from videos. The experimental results are reported in Section 3 and conclusions are drawn in Section 4.
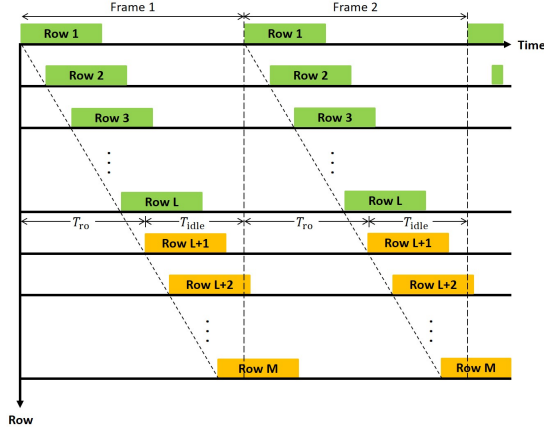
Fig. 1: Illustration of the sample acquisition process of the periodic zero-padding method: Rows 1 to L of each frame are sequentially recorded during the read-out time T_{ro} and the remaining "imaginary" rows' outputs are zeros during the idle period T_{idle}.

2. PROPOSED EXTRACTION METHOD USING PERIODIC ZERO-PADDING

Rolling Shutter Preliminaries The rolling shutter acquires each image over the frame period T_{c} during which each row of the frame is exposed followed by the idle period T_{idle} that no row is captured [13]. The read-out time T_{ro} [14] is defined as the amount of time required for the rows of a frame to be generated and is unique for each camera model. The instantaneous light intensity is captured by all pixels of the same row simultaneously. When the foreground is of uniform color or is removed by motion compensation, the average value of the pixel values in each row is used as a temporal sample, and we refer to the concatenation of these temporal samples as the row signal [13].

In [11], the rolling shutter mechanism was exploited to extract ENF trace from the visual track. During the frame period T_{c}, the rolling shutter can capture M samples to its capacity, among which only L samples recorded during the read-out time T_{ro} will be retained as the rows of each frame. The remaining $M - L$ samples exposed during the idle period T_{idle} will be discarded, where $L \leq M$ and $T_{\mathrm{c}} = T_{\mathrm{ro}} + T_{\mathrm{idle}}$. They concatenate L samples into one single row signal and we refer to this method as the direct concatenation method. The rolling shutter's effective sampling rate F_{s} can be defined in the pair of (M, T_{c}) or (L, T_{ro}) [14] as $F_{\mathrm{s}} = 1/T_{\mathrm{s}} = M/T_{\mathrm{c}} = L/T_{\mathrm{ro}}$, where T_{s} is the amount of time between the start of sampling one row and the start of sampling the subsequent row. In this case, a perceptual sampling frequency $F_{\mathrm{ps}} = L/T_{\mathrm{c}}$ was adopted for the frequency domain analysis without the need of knowing the value of T_{ro}.

Proposed Method In this paper, we propose a periodic zero-padding method for extracting ENF signals from the visual track. Fig. 1 illustrates timing schedule for acquiring the nonzero samples from row 1 to row L and zero samples from
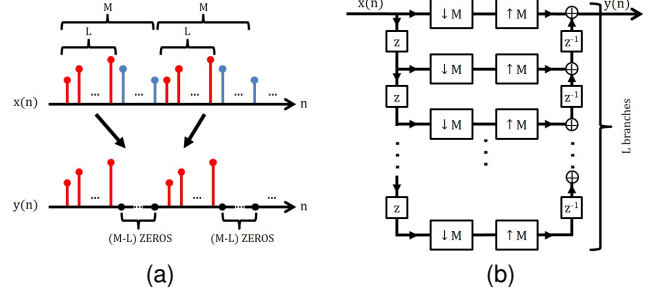
Fig. 2: (a) Time-domain illustration of sample acquisition for the periodic zero-padding method. (b) Equivalent filter bank model with M-fold downsamplers and upsamplers ($L \leq M$).

row $L+1$ to row M. Unlike the direct concatenation method, the estimation of T_{ro} is needed for calculating the value of M via $L \cdot T_{\mathrm{c}}/T_{\mathrm{ro}}$. We denote the time domain input and output signals by $x(n)$ and $y(n)$, respectively, as shown in Fig. 2(a). Out of all M points of the input signal $x(n)$ that corresponds to one frame, we zero out the last $M - L$ samples that correspond to the idle period and denote the resulting output signal as $y(n)$. Such input-output relationship can be modeled by a L-branch filter bank with M-factor downsamplers and upsamplers and unit delay operators, as shown in Fig. 2(b). The DTFT of the lth branch signal can be expressed as follows:

$$Y_l(\omega) = \frac{1}{M}\left(\sum_{m=0}^{M-1} X\left(\omega - \frac{2\pi m}{M}\right) e^{j\left(\omega - \frac{2\pi m}{M}\right)l}\right) e^{-j\omega l}. \tag{1}$$

Hence, the final output $Y(\omega)$ as a summation of all L branches is

$$Y(\omega) = \sum_{l=0}^{L-1} Y_l(\omega) = \sum_{m=0}^{M-1} A_m\, X\left(\omega - \frac{2\pi m}{M}\right), \tag{2}$$

where

$$
\begin{aligned}
A_m &= \frac{1}{M}\sum_{l=0}^{L-1}\exp\left(-j\frac{2\pi m}{M}l\right) \\
&= \frac{L}{M}\mathrm{asinc}_L\left(\frac{2\pi m}{M}\right)\cdot\exp\left(-j\frac{\pi m}{M}(L-1)\right),
\end{aligned} \tag{3}
$$

in which $\mathrm{asinc}_L(x) = \frac{\sin(Lx/2)}{L\sin(x/2)}$ is the *aliased sinc function* or *Dirichlet function* [15]. It is a periodic function that has zero crossings at integer multiples of $\frac{2\pi}{L}$ within one cycle and its maximum values are located at integer multiples of 2π. Replacing the normalized angular frequency ω in (2) by $\frac{2\pi F}{F_{\mathrm{s}}}$, we obtain the output as a function of the analog frequency F as follows:

$$Y(F; F_{\mathrm{s}}) = \sum_{m=0}^{M-1} A_m\, X\left(F - mF_{\mathrm{c}}; F_{\mathrm{s}}\right), \tag{4}$$

where $g(F; F_{\mathrm{s}}) \overset{\text{def}}{=} g(\frac{2\pi F}{F_{\mathrm{s}}})$ for $g = X$ and Y. Eq. (4) shows that $Y(F; F_{\mathrm{s}})$ is the weighted sum of $X(F; F_{\mathrm{s}})$'s that are

shifted by integer multiples of the frame rate $F_c = 1/T_c$. $Y(F; F_s)$ has nonzero ENF frequency components at

$$F = \pm F_e + mF_c + \nu F_s, \tag{5}$$

where $m, \nu \in \mathbb{Z}$ and F_e is defined as the doubled frequency of the nominal ENF. Note that in Eq. (4), the 0th summation term is the ideal input source signal $X(F; F_s)$ scaled by A_0. Observe that the shift step $F_c = F_s/M$, which means that the shifted copies $X(F - mF_c; F_s)$, $m = 0, \cdots, M - 1$ will evenly occupy the full sampling range $[0, F_s)$ Hz. The frequency components that used to be aliased under the slow sampling rate F_c are now well within the range under the rolling shutter's effective sampling frequency F_s.

In order to obtain a high quality extracted ENF signal in terms of the signal-to-noise ratio (SNR), one simple but effective strategy is to pick the frequency component of the highest signal strength, out of the M copies $A_m X(F - mF_c; F_s)$ for $m = 0, \cdots, M - 1$. This is because the noise power is a constant value $(L/M)\sigma^2$, for all frequency components when the input signal $x(n)$ is corrupted by additive white Gaussian noise with power σ^2. Since $|A_m| = \frac{L}{M} \left| \mathrm{asinc}_L \left(\frac{2\pi m}{M} \right) \right|$, the set of elements m^* and k^* which maximizes the SNR or equivalently, $|A_m|$, can be found by the following optimization problem:

$$\min_{m,k \in \mathbb{Z}} \left| \frac{2\pi m}{M} - 2\pi k \right|, \tag{6}$$

which leads to the solution $m^* = Mk^*$. Substituting m^* into (5), we obtain the frequency components of the strongest ENF signals as follows:

$$F_{(m^*, k^*)} = \pm F_e + \left(k^* + \nu \right) F_s, \tag{7}$$

which implies that our proposed method always results in the strongest ENF signal at F_e within the range of $[0, 0.5F_s)$ Hz.

Due to the space limitation, we skip the proof and directly provide the analytic form of the positive frequency component achieving the highest SNR for the direct concatenation method as follows:

$$F_{(m'^*, k'^*, \nu'^*)} = F_e + \mathrm{round}\left((T_{ro} - T_c) F_e \right) F_c + \left(k'^* + \nu'^* \right) F_{ps}, \tag{8}$$

where $\mathrm{round}(x)$ returns the nearest integer of x. It reveals that the direct concatenation method needs both T_c and T_{ro} to determine the location of the shifted frequency component with the strongest ENF signal. Table 1 shows the calculated frequencies that achieve the maximum SNR for the direct concatenation method and our proposed method when $F_e = 120$ Hz and $T_{ro} = 19.8$ ms. The proposed method guarantees that the ENF trace with the highest SNR can always be extracted at the doubled frequency of the nominal ENF, i.e., $F_e = 120$ Hz.

Another advantage of the proposed method over the direct concatenation method is that the Fourier spectrum and

Table 1: Frequency band achieving the maximum SNR.

Case	Frame rate (fps)	Frequency achieving maximum SNR (Hz)	
		Method in [11]	Proposed
1	30.0000	60	
2	23.0062	51	120
3	16.0032	40	

hence the extracted ENF signals are not distorted. Our proposed method has a scaling factor A_m that uniformly scales the magnitude of the ENF signal along the frequency axis, whereas the direct concatenation method has a scaling function $A_{m'}(F)$ [11] that distorts the spectrum along the frequency. However, one should note that such distortion has a minor impact on the quality of the extracted ENF signal as the frequency spread of ENF signals is usually narrow.

3. EXTRACTION OF ENF TRACES

Experimental Conditions We conducted experiments using the back camera of iPhone 6s in an indoor environment with electric lighting in Raleigh, USA. The videos were acquired by facing the mobile camera toward a white wall, and we used the read-out time 19.8 ms reported in [16]. We recorded the power mains signal in parallel and treated it as the ground-truth ENF signal. To calculate a spectrogram for the ENF signal, we split the signal into frames of 12 seconds with 90% overlap. Quadratic interpolation was used to refine the locations of detected spectral peaks [17].

We calculate the SNR at a frequency of interest, F, using the ratio of estimated signal and noise power from the empirical power spectrum within a small neighborhood around F. We estimate the noise power P_{noise} as the averaged power within the frequency ranges $(F - \delta_1, F - \delta_2)$ and $(F + \delta_2, F + \delta_1)$. We estimate the signal power P_{signal} by subtracting the estimate of P_{noise} from the peak power spectrum value at F. In our experiment, we empirically chose $\delta_1 = 2$ Hz and $\delta_2 = 0.5$ Hz.

Results and Discussions Fig. 3 illustrates the spectrogram of the row signal generated by the proposed periodic zero-padding method. In this example, the frame rate of the camera is set to be $F_c = 23.0062$ fps under the nominal value of ENF at 60 Hz to verify whether its spectral composition matches the theoretical prediction. The choice of $F_c = 23.0062$ fps is to avoid the mix of DC and ENF components. In the case of $F_e/F_c \in \mathbb{Z}$, e.g., $F_e = 120$ Hz and $F_c = 30$ fps, DC and ENF from different components will overlap. In Fig. 3(a), we can observe the spectral distribution resulted from the periodic zero-padding method where the multiple DC components appear at intervals of F_c in thick red straps and multiple copies of ENF signal are in faint red straps. Fig. 3(b) shows a zoomed-in region around 120 Hz, where we can see the ENF signals and DC signals appear consistent with the prediction from our theoretical model in Section 2.
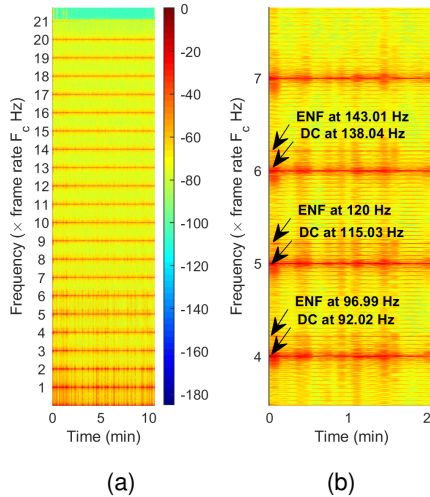
Fig. 3: (a) A spectrogram for the row signal of $F_e = 120$ Hz and $F_c = 23.0062$ fps generated by the proposed periodic zero-padding method. The thick straps are DC components, and the faint straps are the ENF components. (b) Zoomed-in version around 120 Hz.
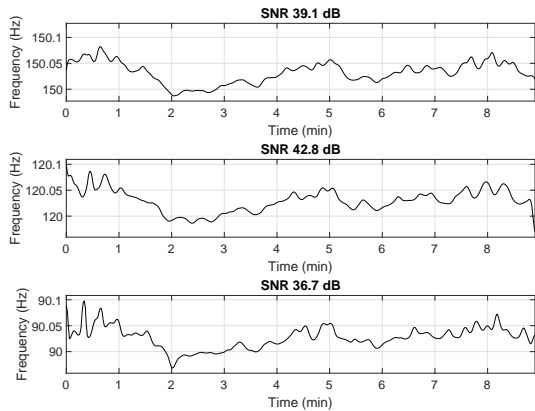

Fig. 4: The ENF signals extracted using the periodic zero-padding method from a static white-wall test video when $F_e = 120$ Hz and $F_c = 30$ fps: [Middle] The ENF signal extracted around $F_e = 120$ Hz achieves the highest SNR; [Top & Bottom] The adjacent ENF signals at 150 Hz and 90 Hz, respectively.

Fig. 4 shows extracted ENF signals from different frequencies when the frame rate is 30 fps, a commonly used sampling rate. The figure reveals that the ENF signal with the highest SNR is achieved at 120 Hz, and the top and bottom plots extracted from the nearest bands at 150 Hz and 90 Hz have lower SNRs. The observation is consistent with the prediction from our theoretical result. It is interesting to note that DC components do not have a strong negative effect on the accuracy of the frequency estimation when overlapping with the ENF components. We plan to investigate the characteristics of the DC components in future work.

To quantitatively compare the extracted ENF signal around 120 Hz of Fig. 4 to the ground-truth ENF signal, we use three matching criteria: the normalized cross-correlation (NCC), the mean squared deviation (MSD), and the mean
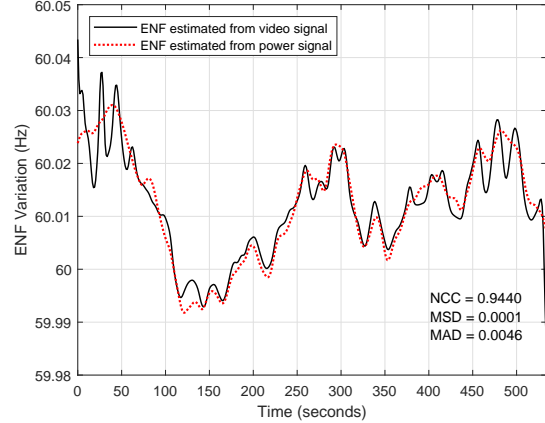

Fig. 5: The ENF trace (black solid) from the maximum SNR of Fig. 4 and its ground-truth ENF signal from power (red dotted). The black ENF trace was properly shifted and scaled to be aligned with the red ENF trace.

Table 2: Comparison of the proposed method with prior art under the low SNR conditions.

SNR (dB)	Average of correlations		p-value
	Method in [11]	Proposed	
-10	0.959	0.951	0.20
-20	0.858	0.892	0.01**
-23	0.754	0.839	0.18
-25	0.459	0.551	0.01**

absolute deviation (MAD). The calculated NCC, MSD, and MAD with respect to the reference signal are shown in Fig. 5. Based on the matching criteria, we confirm that the ENF signal estimate by the periodic zero-padding method is similar to the power reference ENF signal.

To compare the performance of our proposed method with the direct concatenation method [11], we extract ENF signals using the two methods and split each signal into 6 segments to obtain multiple correlation coefficients. We then do a t-test to see if the group means of the correlation coefficients are significantly different in the statistical sense. Table 2 reveals that our proposed method is statistically better than the direct concatenation method at -20 dB and -25 dB, and comparable at -10 dB and -23 dB.

4. CONCLUSION AND FUTURE WORK

In this paper, we have proposed an alternative method for extracting ENF signals by continuing sampling during the idle period. We have analyzed the proposed method using the multirate filter bank model, which shows that the extracted ENF signals are not distorted and the highest SNR component is located at the intrinsic frequency. The experimental results support the theoretical analysis and show that our proposed method can generate more precise ENF signals than the state-of-the-art method. Future work would be conducting extensive evaluations on a large dataset that contains different camera models and SNR conditions.

5. REFERENCES

[1] C. Grigoras, "Applications of ENF criterion in forensic audio, video, computer and telecommunication analysis," *Forensic Science International*, vol. 167, pp. 136–145, Apr. 2007.

[2] D. P. N. Rodríguez, J. A. Apolinário, and L. W. P. Biscainho, "Audio authenticity: Detecting ENF discontinuity with high precision phase analysis," *IEEE Transactions on Information Forensics and Security*, vol. 5, pp. 534–543, Jun. 2010.

[3] M. Kajstura, A. Trawinska, and J. Hebenstreit, "Application of the electrical network frequency (ENF) criterion: A case of a digital recording," *Forensic Science International*, vol. 155, pp. 165–171, Dec. 2005.

[4] A. J. Cooper, "The electric network frequency (ENF) as an aid to authenticating forensic digital audio recordings–an automated approach," in *Audio Engineering Society International Conference on Audio Forensics*, Jun. 2008, pp. 643–661.

[5] S. Vatansever and A. E. Dirik, "Forensic analysis of digital audio recordings based on acoustic mains hum," in *Signal Processing and Communication Application Conference (SIU), 2016 24th*, Jun. 2016, pp. 1285–1288.

[6] X. Lin and X. Kang, "Supervised audio tampering detection using an autoregressive model," in *Acoustics, Speech and Signal Processing (ICASSP), 2017 IEEE International Conference on*, Mar. 2017, pp. 2142–2146.

[7] R. Garg, A. Hajj-Ahmad, and M. Wu, "Geo-location estimation from electrical network frequency signals," in *IEEE International Conference on Acoustics, Speech and Signal Processing*, May 2013, pp. 2862–2866.

[8] A. Hajj-Ahmad, R. Garg, and M. Wu, "ENF-based region-of-recording identification for media signals," *IEEE Transactions on Information Forensics and Security*, vol. 10, pp. 1125–1136, Jun. 2015.

[9] H. Su, A. Hajj-Ahmad, M. Wu, and D. W. Oard, "Exploring the use of ENF for multimedia synchronization," in *IEEE International Conference on Acoustics, Speech and Signal Processing*, May 2014, pp. 4613–4617.

[10] R. Garg, A. L. Varna, A. Hajj-Ahmad, and M. Wu, "' Seeing' ENF: Power-signature-based timestamp for digital multimedia via optical sensing and signal processing," *IEEE Transactions on Information Forensics and Security*, vol. 8, pp. 1417–1432, Jul. 2013.

[11] H. Su, A. Hajj-Ahmad, R. Garg, and M. Wu, "Exploiting rolling shutter for ENF signal extraction from video," in *IEEE International Conference on Image Processing*, Oct. 2014, pp. 5367–5371.

[12] S. Vatansever, A. E. Dirik, and N. Memon, "Detecting the presence of ENF signal in digital videos: A superpixel-based approach," *IEEE Signal Processing Letters*, vol. 24, pp. 1463–1467, Oct. 2017.

[13] H. Su, A. Hajj-Ahmad, C.-W. Wong, R. Garg, and M. Wu, "ENF signal induced by power grid: A new modality for video synchronization," in *ACM International Workshop on Immersive Media Experiences*, Nov. 2014, pp. 13–18.

[14] A. Hajj-Ahmad, A. Berkovich, and M. Wu, "Exploiting power signatures for camera forensics," *IEEE Signal Processing Letters*, vol. 23, pp. 713–717, May 2016.

[15] J. H. McClellan and M. A. Yoder, *DSP first: A multimedia approach*. Prentice Hall PTR, 1997.

[16] C.-W. Wong, A. Hajj-Ahmad, and M. Wu, "Invisible geo-location signature in a single image," in *IEEE International Conference on Acoustics, Speech and Signal Processing*, May 2018, pp. 1987–1991.

[17] K. J. Werner, "The XQIFFT: Increasing the accuracy of quadratic interpolation of spectral peaks via exponential magnitude spectrum weighting," in *International Computer Music Conference*, Sep. 2015, pp. 326–333.